

RADIO EMISSION ON SUB-PARSEC SCALES FROM THE INTERMEDIATE-MASS BLACK HOLE IN NGC 4395

J. M. WROBEL¹ AND L. C. HO²

To appear in the Astrophysical Journal Letters

ABSTRACT

The Seyfert 1 nucleus of NGC 4395 is energized by a black hole of mass $3.6 \times 10^5 M_{\odot}$ (Peterson et al.), making it one of only two nuclear black holes of intermediate mass, $10^3 - 10^6 M_{\odot}$, detected in the radio regime. Building upon UV and X-ray evidence for outflows from this Seyfert nucleus, the VLBI High Sensitivity Array was used at 1.4 GHz to search for extended structure on scales greater than 5 mas (0.1 pc). Elongated emission was discovered, extending over 15 mas (0.3 pc) and suggesting an outflow on sub-parsec scales from this intermediate-mass black hole. The Seyfert nucleus is located at the center of an elliptical star cluster, and the elongation position angle of the sub-parsec radio structure is only 19° from the star cluster's minor axis.

Subject headings: galaxies: active — galaxies: individual (NGC 4395) — galaxies: nuclei — galaxies: Seyfert — radio continuum: galaxies

1. MOTIVATION

Dynamical studies have established that supermassive black holes, with masses $10^6 - 10^9 M_{\odot}$, occur in the nuclei of most nearby galaxies with stellar bulges. The focus has now turned to searches for intermediate-mass black holes (IMBHs), with masses $10^3 - 10^6 M_{\odot}$, in nearby galactic nuclei. Finding IMBHs will help to define the nature of the seed black holes that figure in models for the growth of black holes over cosmic time and to predict the gravitational radiation background expected for *LISA* due to mergers of IMBHs. In this mass regime, dynamical searches currently fail beyond the Local Group and are being replaced by surveys for signatures of active galactic nuclei (AGN; Greene & Ho 2004). Such AGN searches are strongly guided by the discovery of a candidate IMBH in NGC 4395 (Filippenko & Ho 2003), recently established as a bona fide nuclear IMBH with mass $(3.6 \pm 1.1) \times 10^5 M_{\odot}$ (Peterson et al. 2005).

NGC 4395 is a bulgeless Sdm galaxy at a Cepheid distance of 4.3 ± 0.3 Mpc with a scale 0.021 pc mas⁻¹ (Thim et al. 2004). Its nucleus has the emission properties of a Seyfert 1, with broad permitted optical and UV emission lines (Filippenko, Ho, & Sargent 1993; Filippenko & Ho 2003; Peterson et al. 2005) and a pointlike, hard X-ray source that is highly time-variable (Shih, Iwasawa, & Fabian 2003; Moran et al. 2005; Vaughan, et al. 2005). The reverberation study by Peterson et al. (2005) reports a characteristic diameter for the UV broad-line-region (BLR) of 7.0×10^{-5} pc or 0.0033 mas. There are hints of an outflowing UV absorber close to the nucleus of this AGN (Crenshaw et al. 2004). Also, in luminous AGNs, warm X-ray absorbers close to the nucleus are often associated with outflows; in NGC 4395 such absorbers have been inferred from variations in their ionization (Shih, Iwasawa, & Fabian 2003) and/or column densities (Moran et al. 2005). While these X-ray and UV hints of outflows are intriguing, seek-

ing structural evidence for an outflow is an essential next step.

NGC 4395 is one of only two nuclear IMBHs that have been detected in the radio regime (Greene, Ho, & Ulvestad 2006), important because VLBI on mas scales can then be used to search for structural evidence for an outflow on sub-parsec scales. At 1.4 GHz, the Very Long Baseline Array (VLBA; Napier et al. 1994) detected one source, with flux density 0.53 ± 0.13 mJy, spectral power 1.2×10^{18} W Hz⁻¹, diameter less than 11 mas (0.2 pc), and brightness temperature more than 2 million K (Wrobel, Fassnacht, & Ho 2001). While these traits are consistent with the VLBA detection being accretion-powered by the IMBH, the resolution and sensitivity of the VLBA image failed to provide quantitative structural information. This Letter reports improved imaging of the Seyfert nucleus of NGC 4395 at 1.4 GHz, using a VLBI High Sensitivity Array (HSA) consisting of the VLBA, the Very Large Array (VLA; Thompson et al. 1980) operating in its phased mode, and the Robert C. Byrd Green Bank Telescope (GBT; Jewell & Prestage 2004).³ The HSA imaging is described in Section 2. The implications for the Seyfert nucleus are explored in Section 3, with an emphasis on the discovery of elongated structure on sub-parsec scales.

2. HSA IMAGING

The HSA was used to observe NGC 4395 and calibrators on 2005 May 1 0000-0800 UT. Data were acquired in dual circular polarizations with 4-level sampling and at a center frequency of 1.43849 GHz with a bandwidth per polarization of 32 MHz, formed from four contiguous baseband channels each of width 8 MHz. Antenna separations spanned 50-8600 km. Phase-referenced observations were made in the nodding style. A 200 s observation of NGC 4395 was preceded and followed by a 100 s observation of the phase, rate, and delay cal-

¹ National Radio Astronomy Observatory, P.O. Box O, Socorro, NM 87801; jwrobel@nrao.edu

² The Observatories of the Carnegie Institution of Washington, 813 Santa Barbara Street, Pasadena, CA 91101; lho@ociw.edu

³ The VLBA, the VLA, and the GBT are operated by the National Radio Astronomy Observatory, which is a facility of the National Science Foundation, operated under cooperative agreement by Associated Universities, Inc.

ibrator J1220+3431 about 1.5° from NGC 4395. Observation and correlation assumed a coordinate equinox of 2000. All *a priori* calibrator positions were taken from the Goddard VLBI global solution 2004 f, ⁴ and had one-dimensional errors at 1σ better than 1 mas. The *a priori* position for NGC 4395 was from Wrobel, Fassnacht, & Ho (2001) after adjusting for the solution 2004 f position for J1220+3431.

Data editing, calibration, and imaging were done using the 2005 December 31 release of the NRAO AIPS software, following strategies outlined in the AIPS Cookbook⁵. Correlation was affected by inappropriate Earth Orientation Parameters, so corrections to those parameters were made (Walker et al. 2005). Data deletion was based on system flags recorded at observation and media weights recorded at correlation. Data compromised by radio frequency interference were also deleted, as were data on baselines involving any antenna observing below an elevation of 20° . For NGC 4395, these steps yielded a total integration time of 4 hr. Corrections for the dispersive delays caused by the Earth’s ionosphere were made using electron-content models from the Jet Propulsion Laboratory. Ancillary HSA data were used to set the amplitude scale to an accuracy of about 5%, after first correcting for sampler errors. The visibility data for J1220+3431 were used to generate phase-referenced visibility data for NGC 4395 and for the check source J1215+3448, observed to assess both the differential astrometry and the coherence losses. All calibrators were phase-self-calibrated. No self-calibrations were performed on NGC 4395. No polarization calibration was performed, as only an upper limit on the linear polarization percentage of NGC 4395 was sought. AIPS task *imagr* was used to image all calibrators in Stokes *I* and NGC 4395 in Stokes *I*, *Q*, and *U*.

The visibility data for NGC 4395 were imaged with natural weighting, achieving the expected theoretical rms noise within the field-of-view limits set by time and bandwidth averaging. The most constraining limit follows from accepting, at the field edge, a 5% drop in the peak amplitude due to averaging over each 8 MHz baseband channel; the resulting field-of-view diameter is about 590 mas. A region of diameter 550 mas (12 pc) was searched in Stokes *I* to match the upper limit of the unresolved VLA detection (Ho & Ulvestad 2001). The Seyfert nucleus was easily detected above 5σ in the cleaned image and found to be slightly extended, with an integrated flux density of 0.74 ± 0.04 mJy being recovered (Fig. 1, left). There were also hints of 5σ emission about 250 mas (5.2 pc) to the west of the nucleus. Nothing else was detected in Stokes *I* above 5σ or a brightness temperature threshold of 250,000 K. Nothing was detected in Stokes *Q* or *U* so those images were not cleaned. Near the Seyfert nucleus, the image of linearly polarized intensity $P = \sqrt{Q^2 + U^2}$ revealed no emission above 5σ , implying an upper limit of 2% in the polarization percentage.

The visibility data for NGC 4395 were also imaged with a “robustness” parameter of -0.3 for an optimal balance between resolution and sensitivity (Briggs 1995). Guided by the 4σ contours in the cleaned Stokes *I* image (Fig. 1,

right), emission extends from the peak for about 15 mas (0.3 pc) along a position angle (PA) of about 28° . Analysis of the check source J1215+3448, observed 0.9° from J1220+3431 and imaged with the same robustness, implied a correction of about 2% for residual errors in the phase calibration and a one-dimensional error of about 3 mas in the differential astrometry. NGC 4395 was observed 1.5° from J1220+3431, so for that still-desirable geometry these corrections are conservatively doubled to about 4% and 6 mas, respectively. A quadratic fit to the peak in the right panel of Figure 1 gave a corrected value of 0.24 mJy beam⁻¹ and a position of $\alpha(J2000) = 12^h 25^m 48^s.8774$ and $\delta(J2000) = 33^\circ 32' 48''.715$, with a one-dimensional error of 6 mas (the quadratic sum of the errors due to the signal-to-noise ratio, in the position for J1220+3431, and in the differential astrometry).

A standard analysis of the data from the internal VLA baselines yielded an integrated flux density of 1.69 ± 0.08 mJy with a deconvolved diameter of less than $2''$ (42 pc), plus no evidence for adjacent emission on larger scales. For comparison, Ho & Ulvestad (2001) reported an integrated flux density of 1.68 ± 0.09 mJy with a deconvolved diameter of less than 550 mas (12 pc) on 1999 Aug 29 UT, and a spectral index $\alpha = -0.60 \pm 0.08$ ($S \propto \nu^\alpha$) between 1.4 and 4.9 GHz. The HSA imaging thus recovers about 0.4 of the flux density available at 1.4 GHz.

3. IMPLICATIONS AND FUTURE DIRECTIONS

The IMBH that energizes the Seyfert nucleus in NGC 4395 has an Eddington ratio of only $\sim 1.2 \times 10^{-3}$ (Peterson et al. 2005). By analogy with supermassive black holes and stellar-mass black holes, such an Eddington ratio suggests that this IMBH is in a low/hard or quiescent state and, thus, is expected to launch a steady polar outflow (Ho 2005; Jester 2005; Nagar et al. 2005; Narayan 2005). The elongated structure in Figure 1 is indeed suggestive of a radio outflow on sub-parsec scales from the IMBH in NGC 4395. This radio structure extends for about 15 mas (0.3 pc) along a PA of about 28° . From the observed smoothness of the H α line, Laor et al. (2006) suggest that the BLR gas is structured as a smooth, rotationally-dominated flow, most likely in a geometrically thick configuration. This geometrically thick structure may be involved in launching the suspected radio outflow.

For perspective, 20 of the 44 low-luminosity AGN (LLAGN) surveyed at mas resolution by Nagar et al. (2005) do show structure on sub-parsec scales. Six of those 20 have sub-parsec scale structures with weak or no known larger scale jets, perhaps because the jet does not propagate beyond the inner few parsecs. For NGC 4395 at 1.4 GHz, the VLA source lacks adjacent emission and has the same integrated flux densities for deconvolved sizes of 10-40 pc, whereas the HSA imaging traces a suspected outflow on sub-parsec scales. Given these VLA and HSA properties, NGC 4395 can now be added to the subset of LLAGN whose emission does not extend beyond the inner few parsecs. The spectral power of the emission recovered in the left panel of Figure 1 is $P_{1.4} = 1.6 \times 10^{18}$ W Hz⁻¹, while that for the corrected peak in the right panel of Figure 1 is $P_{1.4} = 5.3 \times 10^{17}$ W Hz⁻¹. As expected, these powers bracket the value derived from the VLBA discovery

⁴ http://gemini.gsfc.nasa.gov/solutions/2004f_astro/

⁵ <http://www.aoc.nrao.edu/aips/cook.html>

image (Wrobel, Fassnacht, & Ho 2001). The sub-parsec scale of the suspected outflow in NGC 4395 corresponds to 10^7 Schwarzschild radii, very different from the upper limits of 10^3 to 10^4 Schwarzschild radii inferred for several LLAGN with flat radio spectra (Anderson et al. 2004).

The potential importance of outflows in mediating black-hole growth has been highlighted by Pellegrini (2005), motivating an estimate of the kinetic luminosity of the suspected outflow from NGC 4395. But unless the environs of the LLAGN are spatially resolved, such estimates can be very model-dependent. The environs of the LLAGN in M51, at a distance of 8.4 Mpc, are spatially resolved in the radio, optical, and X-ray regimes (Terashima & Wilson 2001). Moreover, VLA imaging at 1.4 GHz shows that the LLAGN in M51 is only eight times as powerful as the LLAGN in NGC 4395, and similarly compact (Ho & Ulvestad 2001). For M51, Terashima & Wilson (2001) estimate that the kinetic luminosity of its jet is comparable to the bolometric luminosity of its LLAGN. For NGC 4395, the bolometric luminosity of its LLAGN is $\sim 5.4 \times 10^{40}$ ergs s^{-1} (Peterson et al. 2005), so by analogy with M51, a kinetic luminosity of this order could be available within the inner few parsecs of NGC 4395. Approximating the radio luminosity of NGC 4395 as the product of the frequency times power, the luminosity of the emission recovered in the left panel of Figure 1 is $L_{1.4} = 2.4 \times 10^{34}$ ergs s^{-1} , while that for the corrected peak in the right panel of Figure 1 is $L_{1.4} = 7.6 \times 10^{33}$ ergs s^{-1} . Although these radio luminosities are about six orders of magnitude below the bolometric luminosity of the Seyfert nucleus, the HSA imaging helps set a characteristic length scale for the available kinetic luminosity.

The absorption-corrected, time-averaged 2-10 KeV luminosity of the Seyfert nucleus in NGC 4395 is $L_X = 8.8 \times 10^{39}$ ergs s^{-1} (Moran et al. 2005). Combining this with the 5-GHz luminosity of $L_5 = 8.8 \times 10^{34}$ ergs s^{-1} (Ho & Ulvestad 2001), the nucleus of NGC 4395 is formally radio-quiet, with $\log(L_5/L_X) = -5$ (Terashima & Wilson 2003). Similarly, the nucleus is formally radio-quiet when cast in terms of its radio-to-optical ratio (Greene, Ho, & Ulvestad 2006). Still, this Seyfert nucleus seems able to support a radio outflow, suggesting that the physically defining characteristic is the Eddington ratio of its energizing IMBH. Hence while NGC 4395 can be classed as a narrow-line Seyfert 1 galaxy energized by an IMBH, its radio properties might be expected to differ from those for a sample of similar galaxies selected to have Eddington ratios near unity (Greene, Ho, & Ulvestad 2006).

The PA of the sub-parsec scale radio structure, about 28° , can be compared to the other nuclear structures in NGC 4395 imaged at lower resolution with the *Hubble Space Telescope* (HST; Filippenko, Ho, & Sargent 1993; Matthews et al. 1999; Filippenko & Ho 2003). In a WFPC2 I-band image, the Seyfert nucleus is located at the photometric center of a nuclear star cluster with a half-light diameter of 380 mas (8.0 pc), an axis ratio of 0.83, and a minor-axis PA of 9° (Filippenko & Ho 2003), confirming the earlier findings in the I band by Matthews et al. (1999). In contrast, the galactic disk has a minor-axis PA of 54° as traced by HI (Swaters et al. 1999) and 57° as traced by starlight (Ho & Ulvestad

2001). The elongation PA of the sub-parsec radio structure in NGC 4395 is thus closer to the minor axis of the star cluster than that of the galactic disk. But the significance of this is unclear, given the propensity of jet directions in Seyfert galaxies to be uncorrelated with the minor axes of their galactic disks (Kinney et al. 2000).

In a WFPC F502N image centered on the [OIII] $\lambda 5007$ line, the nuclear structure is somewhat resolved with emission-line gas extending to the west of the Seyfert nucleus (Filippenko, Ho, & Sargent 1993). Using their WFPC2 B-band and I-band images, Matthews et al. (1999) do find evidence for two structures to the west, namely a small blue arc offset by 250 mas (5.2 pc) and an extended blue plume offset by about $1''$ (21 pc). Matthews et al. (1999) argue that these two blue features are probably due to [OIII] emission from gas within a nuclear ionization cone. The opening angle of the cone structure covers PAs of $265\text{--}280^\circ$, whereas the sub-parsec scale radio structure defines PAs of about $28/208^\circ$. The relation between these two structures is not presently understood, perhaps due to projection effects for both structures.

The naturally-weighted HSA image shows hints of 5σ emission about 250 mas (5.2 pc) to the west of the nucleus, thus in the vicinity of the small blue arc reported by Matthews et al. (1999). The reality of this faint extranuclear emission at 1.4 GHz is, at present, far from certain. But if it is real, it has peak brightness temperatures above 250,000 K in the vicinity of probable [OIII] emission (Matthews et al. 1999). As the HSA imaging of the nucleus has recovered only about forty percent of the flux density available at 1.4 GHz, the faint extranuclear emission could be providing the first clues about the location of the approximately 1 mJy still missing from the HSA image. HSA imaging with higher sensitivity could test the reality of the faint extranuclear emission and should be done. Also, *HST* spectroscopic imaging of the small blue arc and the extended blue plume discovered by Matthews et al. (1999) should be done to test the suggestion by those authors that these blue structures trace [OIII] emission.

The nuclear star clusters in other late-type spiral galaxies are in most respects very similar to that in NGC 4395, and within each star cluster a mixture of stellar populations of different ages is found, suggesting a prolonged formation period (Walcher et al. 2006). For NGC 4395, few constraints on the cluster's stellar populations are available. Filippenko, Ho, & Sargent (1993) find no UV evidence for the P Cygni profiles that would be expected from winds from massive OB stars. Filippenko & Ho (2003) do detect the calcium infrared triplets, indicating that red supergiants are present. The half-light diameter of the nuclear star cluster is 380 mas (8.0 pc), so the HSA imaging samples most of the cluster's volume. To further constrain the stellar populations, as well as to assist with the radio-optical registration, the naturally-weighted HSA image was searched for cluster emitters within the half-light diameter. None were found above a peak flux density of 0.05 mJy per beam, corresponding to a brightness temperature threshold of 250,000 K and a power threshold of $P_{1.4} = 1.1 \times 10^{17}$ W Hz^{-1} . For comparison, an analog to the radio counterpart to an ultraluminous X-ray source, at a distance of 4.8 Mpc in NGC 5408 (Kaaret et al. 2003), would emit at the 0.3-

mJy level at 4.8 GHz at the distance of NGC 4395. Such emission would be consistent with the VLA photometry of NGC 4395 at 4.9 GHz (Ho & Ulvestad 2001). However, given its steep-spectrum nature, such a radio analog would be boosted well above the HSA detection threshold at 1.4 GHz and, thus, cannot be present within the star cluster's half-light diameter. HSA imaging with higher

sensitivity would help constraint other classes of cluster emitters.

The authors thank J. Ulvestad for useful feedback on the draft manuscript.

Facilities: GBT, VLA, VLBA.

REFERENCES

- Anderson, J. M., Ulvestad, J. S., & Ho, L. C. 2004, *ApJ*, 603, 42
 Briggs, D. S. 1995, Ph. D. thesis, New Mexico Institute of Mining and Technology
 Crenshaw, D. M., et al. 2004, *ApJ*, 612, 152
 Filippenko, A. V., Ho, L. C., & Sargent, W. L. W. 1993, *ApJ*, 410, L75
 Filippenko, A. V., & Ho, L. C. 2003, *ApJ*, 588, L13
 Greene, J. E., & Ho, L. C. 2004, *ApJ*, 610, 722
 Greene, J. E., Ho, L. C., & Ulvestad, J. S. 2006, *ApJ*, 636, 56
 Ho, L. C. 2005, *Ap&SS*, 300, 219
 Ho, L. C., & Ulvestad, J. S. 2001, *ApJS*, 133, 77
 Jester, S. 2005, *ApJ*, 625, 667
 Jewell, P. R., & Prestage, R. M. 2004, *SPIE*, 5489, 312
 Kaaret, P., Corbel, S., Prestwich, A. H., & Zezas, A. 2003, *Science*, 299, 365
 Kinney, A. L., Schmitt, H. R., Clarke, C. J., Pringle, J. E., Ulvestad, J. S., & Antonucci, R. R. J. 2000, *ApJ*, 537, 152
 Laor, A., Barth, A. J., Ho, L. C., & Filippenko, A. V. 2006, *ApJ*, 636, 83
 Matthews, L. D., et al. 1999, *AJ*, 118, 208
 Moran, E. C., Eracleous, M., Leighly, K. M., Chartas, G., Filippenko, A. V., Ho, L. C., & Blanco, P. R. 2005, *AJ*, 129, 2108
 Nagar, N. M., Falcke, H., & Wilson, A. S. 2005, *A&A*, 435, 521
 Napier, P. J., Bagri, D. S., Clark, B. G., Rogers, A. E. E., Romney, J. D., Thompson, A. R., & Walker, R. C. 1994, *Proc. IEEE*, 82, 658
 Narayan, R. 2005, *Ap&SS*, 300, 177
 Pellegrini, S. 2005, *ApJ*, 624, 155
 Peterson, B. M., et al. 2005, *ApJ*, 632, 799
 Shih, D. C., Iwasawa, K., Fabian, A. C. 2003, *MNRAS*, 341, 973
 Swaters, R. A., Shoenmakers, R. H. M., Sancisi, R., & van Albada, T. S. 1999, *A&A*, 304, 330
 Terashima, Y., & Wilson, A. S. 2001, *ApJ*, 560, 139
 Terashima, Y., & Wilson, A. S. 2003, *ApJ*, 583, 145
 Thim, F., Hoessel, J. G., Saha, A., Claver, J., Dolphin, A., & Tammann, G. A. 2004, *AJ*, 127, 2322
 Thompson, A. R., Clark, B. G., Wade, C. M., Napier, P. J., 1980, *ApJS*, 44, 151
 Vaughan, S., Iwasawa, K., Fabian, A. C., & Hayashida, K. 2005, *MNRAS*, 356, 524
 Walcher, C. J., Boker, T., Charlot, S., Ho, L. C., Rix, H.-W., Rossa, J., Shields, J. C., & van der Marel, R. P. 2006, *ApJ*, submitted (astro-ph/0604138)
 Walker, R. C., Dhawan, V., Brisken, W., Benson, J., Kogan, L., & Romney, J. 2005, VLBA Test Memo 69
 Wrobel, J. M., Fassnacht, C. D., & Ho, L. C. 2001, *ApJ*, 553, L23

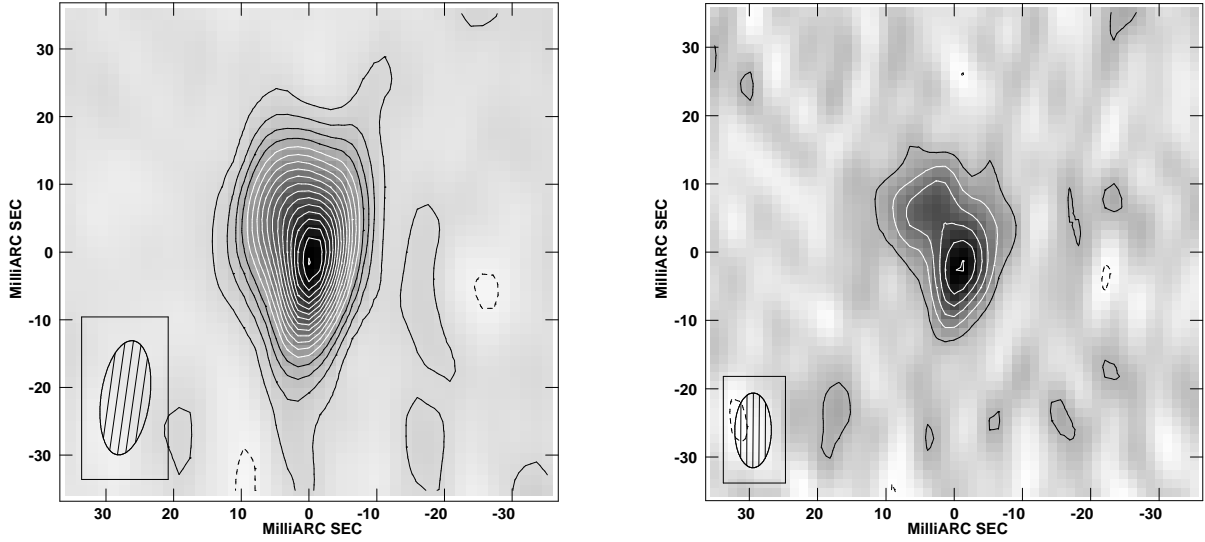


FIG. 1.— HSA images of Stokes I emission from NGC 4395 at a frequency of 1.4 GHz, centered on the *a priori* observation position, and spanning 70 mas (1.5 pc) per coordinate. Negative contours are dashed and positive ones are solid. *Left*: Natural weighting, giving an rms noise of $0.010 \text{ mJy beam}^{-1}$ (1σ) and beam dimensions at FWHM of 17 mas (0.4 pc) by 7.2 mas (0.2 pc) with elongation PA -8° (hatched ellipse). Linear grey scale spans $-0.04 \text{ mJy beam}^{-1}$ to the peak of $0.36 \text{ mJy beam}^{-1}$. Contours are at $-6, -4, -2, 2, 4, 6, 8, 10, 12, 14, \dots, 36$ times σ . *Right*: Robustness parameter of -0.3 , giving an rms noise of $0.019 \text{ mJy beam}^{-1}$ (1σ) and beam dimensions at FWHM of 11 mas (0.2 pc) by 5.4 mas (0.1 pc) with elongation PA 0° (hatched ellipse). Linear grey scale spans $-0.04 \text{ mJy beam}^{-1}$ to the peak of $0.23 \text{ mJy beam}^{-1}$. Contours are at $-6, -4, -2, 2, 4, 6, 8, 10,$ and 12 times σ .